Formation and repair of an interstrand DNA cross-link arising from a common endogenous lesion

Kurt Housh,[§] Jay S. Jha,[§] Zhiyu Yang,[§] Tuhin Haldar,[§] Kevin M. Johnson,[§] Jiekai Yin,[†] Yinsheng Wang[†] and Kent S. Gates[§,‡,*]

[§]University of Missouri
Department of Chemistry
125 Chemistry Building
Columbia, MO 65211, United States

[‡]University of Missouri
Department of Biochemistry
125 Chemistry Building
Columbia, MO 65211, United States

[†]Department of Chemistry
University of California-Riverside
Riverside, California 92521-0403, United States

* To whom correspondence should be addressed: email: gatesk@missouri.edu; Tel.: (573) 882-6763

Abstract: Interstrand DNA cross-links (ICLs) are cytotoxic because they block the strand separation required for read-out and replication of the genetic information in duplex DNA. The unavoidable formation of ICLs in cellular DNA may contribute to aging, neurodegeneration, and cancer. Here we describe the formation and properties of a structurally complex ICL derived from an apurinic/apyrimidinic (AP) site, which is one of the most common endogenous lesions in cellular DNA. The results characterize a cross-link arising from aza-Michael addition of the N^2-amino group of a guanine residue to the electrophilic sugar remnant generated by spermine-mediated strand cleavage at an AP site in duplex DNA. An α,β-unsaturated iminium ion is the critical intermediate involved in ICL formation. Studies employing the bacteriophage ϕ29 polymerase provided evidence that this ICL can block critical DNA transactions that require strand separation. The results of biochemical studies suggest that this complex strand break/ICL might be repaired by a simple mechanism in which the 3'-exonuclease action of the enzyme apurinic/apyrimidinic endonuclease (APE1) unhooks the cross-link to initiate repair via the single-strand break repair pathway.

INTRODUCTION

The sequence of nucleobases in DNA provides the genetic code that is critical for all living organisms.[1] From a chemical perspective, DNA displays impressive stability. For example, it has been possible to recover sequence information from DNA samples that are more than 1,000,000 years old.[2-3] Indeed, intrinsic chemical stability is one of the properties that makes DNA a candidate for next-generation digital information storage.[4-5] Spontaneous DNA degradation reactions such as phosphodiester hydrolysis, cytosine deamination, and hydrolysis of the *N*-glycosidic bonds that hold purine residues to the DNA backbone are very slow, with half-lives of 3×10^7 y, 3×10^5 y, and 7.5×10^2 y, respectively.[6-9] Nonetheless, in the context of a diploid human cell containing 12.6 billion nucleotides,[10] some of these reactions can produce potentially harmful numbers of DNA lesions. For example, the spontaneous loss of purine residues introduces 10,000 apurinic (AP) sites per day into the DNA of each cell.[8-9, 11] Enzymatic reactions further increase the cellular load of AP sites and other DNA lesions.[12-14]

Unavoidable, endogenous DNA damage has important biological consequences.[15-16] Replication of a damaged DNA template can lead to mutations and other types of genetic instability.[15, 17] Such genetic changes drive the evolution of species[18] but, in the context of individual organisms, are generally detrimental.[19] The requirement for genetic stability in living organisms led to the evolution of proteins that repair the unavoidable damage sustained by cellular DNA.[20]

Interstrand cross-links (ICLs) are a particularly problematic form of DNA damage. Covalent connection of the two strands in duplex DNA blocks readout and replication of genetic information.[21-22] Complex and resource-intensive pathways exist

for the removal of ICLs from cellular DNA[23-26] but the identity of the endogenous cross-links that serve as the natural substrates for these repair pathways remains uncertain.[27-29] Defects in ICL repair proteins are associated with cancer, neurodegeneration, and accelerated aging.[16, 28, 30-31] Deeper understanding of the formation, consequences, and repair of endogenous cellular ICLs may provide insights regarding the fundamental processes that drive disease and determine healthspan in humans.

Our work describes the formation and properties of a potential endogenous cross-link derived from a ubiquitous endogenous lesion found in the DNA of all organisms. Specifically, we find that amine-catalyzed cleavage of abasic sites in duplex DNA can give rise to an interstrand cross-link adjacent to a strand break. The results indicate that cross-link formation involves conjugate addition of the N^2-amino group of a guanine residue to the electrophilic α,β-unsaturated iminium ion intermediate generated during spermine-catalyzed β-elimination at an AP site in duplex DNA. Our biochemical studies provide evidence that the ICL can block critical DNA transactions such as replication and transcription, but also offer the possibility that this complex lesion may be repaired by a remarkably simple pathway in which the 3'-exonuclease action of the enzyme apurinic/apyrimidinic endonuclease (APE1) unhooks the ICL. This unprecedented activity of APE1 may enable repair to proceed through a variant of the single-strand break repair pathway[32] rather than the more arduous routes offered by classical ICL repair pathways.[23-24]

BACKGROUND

Secondary Lesions Generated from Abasic (AP) Sites in Duplex DNA. AP sites are among the most common endogenous lesions in cellular DNA.[8-9, 33-35] In duplex DNA, AP sites exist as an equilibrating mixture of the ring-closed hemiacetal alongside small amounts of the ring-opened aldehyde (~1%, Scheme 1).[36] Reactivity associated with the ring-opened aldehyde form of the AP residue leads to the generation of secondary lesions including ICLs[37-41] and DNA-protein cross-links.[42-43]

Of special relevance to the present work, the reaction of the AP aldehyde residue with the N^2-amino group of a guanine residue on the opposing strand can generate an imine-derived DNA-DNA ICL (dG-AP, Schemes 2 and 3).[39, 44-45] When this cross-linking reaction is carried out in the presence of the reducing agent $NaBH_3CN$, higher yields of an N^2-alkylguanine ICL are generated via a reductive amination process (dG-AP_{red}, Scheme 2).[39, 44-45] This type of "full-size" cross-linked duplex (containing both unbroken, full-length strands of the starting duplex) was employed as a size-marker in some of the gel electrophoretic experiments reported below.

The acidic nature of the α-protons[46] in the ring-opened aldehyde enables the conversion of AP sites into DNA strand breaks via β-elimination of the 3'-phosphoryl group (Scheme 1).[47-49] Spontaneous strand cleavage at AP sites in neutral aqueous buffer is slow, taking place with a half-life of 8-40 d in pH 7 buffer at 37 ˚C.[48, 50] The rate of this reaction is increased at high temperature.[51] Biological amines can also catalyze strand cleavage at AP sites in DNA via obligate iminium ion intermediates (Scheme 1).[48-50, 52-59] Importantly, strand cleavage involving β-elimination at an AP site in DNA generates an electrophilic *trans*-α,β-unsaturated aldehyde sugar remnant on the 3'-

terminus of the strand break (Scheme 1).[56-57] This *trans*-α,β-unsaturated aldehyde sugar remnant residue has been detected in the DNA of cultured human cells[47] and is one of the few examples of an α,β-unsaturated aldehyde generated by endogenous cellular processes.[60]

Various names and abbreviations have been used when referring to the *trans*-α,β-unsaturated aldehyde sugar remnant generated by β-elimination at an AP site in DNA. These include: *trans*-4-hydroxypent-2-enal 5-phosphate, βE (β-elimination product),[47] 3'dRP (3'deoxyribose phosphate),[61] 3'ddR5P (2,3-didehydro-2,3-dideoxy-ribose-5-phosphate),[54, 62] and 3'PUA (phospho-α,β-unsaturated aldehyde).[43, 63] Here we will use the 3'PUA nomenclature.

In subsequent sections, we present evidence for generation of an ICL by reaction of a guanine residue with the electrophilic 3'α,β-unsaturated iminium ion intermediate produced by amine-catalyzed cleavage of an AP in duplex DNA.

RESULTS AND DISCUSSION

Generation of DNA Duplexes Containing AP-derived Strand Breaks at Defined Locations. DNA duplexes containing AP sites at defined locations were generated by treatment of the corresponding 2'-deoxyuridine (dU)-containing duplexes with the enzyme uracil DNA glycosylase (UDG).[12, 39, 64-65] This is a biomimetic process mirroring a major pathway for the formation of AP sites in eukaryotic cells.[13-14, 66]

In these studies, strand cleavage at AP sites was induced by a variety of established methods.[9] Heating at 95 ˚C for 1 h in HEPES buffer (50 mM, pH 7.4) containing NaCl (100 mM) was used to generate a mixture of the 3'PUA and 3'phosphate

cleavage products in 66±20% yield, alongside the intact AP-containing duplex.[51] Treatment of AP-containing DNA duplexes with NaOH (165 mM, 37 °C, 30 min) similarly was used to convert the AP site into a mixture of the 3'PUA and 3'phosphate cleavage products.[67] Likewise, treatment with piperidine (1 M, 95 ˚C, 25 min) induced conversion of the AP oligonucleotide to a mixture of the 3'PUA and 3'phosphate cleavage products.[53, 68-69]

In some experiments, the base excision repair enzyme endonuclease III (Endo III or Nth) was used to induce cleavage of AP sites in duplex DNA. While it is widely reported that Endo III generates the 3'PUA cleavage product,[57, 70] several studies have provided evidence that the combined glycosylase-lyase action of this enzyme, in fact, generates the 3'deoxyribose cleavage product (3'dR, Scheme 1) generated by formal conjugate addition of water to the 3'PUA group.[66, 71-72] We employed gel electrophoretic and mass spectrometric analyses to provide evidence that the lyase action of Endo III on AP-containing DNA duplexes generates the 3'dR cleavage product (Figure S2**)**.

Finally, in the experiments that are the focus of this work, strand cleavage (and accompanying ICL formation) was induced by physiologically-relevant concentrations (1 mM) of the biogenic amine spermine.[48-49, 52-54] Spermine has a variety of functions in mammalian cells including DNA compaction in the nucleus.[52, 73-76]

Gel Electrophoretic Evidence That Amine-catalyzed Strand Cleavage of the AP Site in DNA Duplex A Generates an ICL. The AP-containing strand in duplex **A** was labeled with a 5'-^{32}P-phosphoryl group to enable monitoring of strand-cleavage and ICL formation. The products arising from this AP-containing duplex under various conditions

were resolved by electrophoresis on 20% denaturing polyacrylamide gels and the radioactivity in each band quantitatively measured by storage phosphor autoradiography.[77] In denaturing gel electrophoretic analyses, ICLs appear as slow-migrating bands, located above the uncross-linked AP-containing oligodeoxynucleotide in the gel images shown here.[39-40, 78] The smaller DNA fragments arising from cleavage of the oligodeoxynucleotide at the AP site appear as fast-migrating bands near the bottom of the gel images.

Successful generation of the AP site in duplex **A** was confirmed by NaOH workup to induce cleavage of the AP-containing strand into smaller, fast-migrating products (Figure 1, lane 2). Incubation of the AP-containing duplex **A** in pH 7.4 buffer led to a low yield (approximately 1%) of a slow-migrating product consistent with the "full-size" dG-AP ICL described previously (Figure 1, lane 5 and Figure S3).[39] As expected, incubation of the AP-containing duplex in sodium acetate buffer (750 mM, pH 5.2) containing $NaBH_3CN$ (250 mM) produced a larger yield of slow-migrating product (7±1%, Figure 1, lane 6) consistent with the full-size dG-AP_{red} ICL derived from reductive amination (duplex **B**, Figure 1 and Scheme 3).[39] The full-size cross-linked duplex **B** served as a useful size-marker in our characterization of the ICL induced by spermine-mediated strand cleavage of the AP site in duplex **A** described below.

Incubation of duplex **A** with spermine (1 mM) in HEPES buffer (50 mM, pH 7.4 containing 100 mM NaCl) for 24 h at 37 ˚C generated a substantial yield of a slow-migrating band in the gel (31±3%, lane 7 of Figure 1) accompanied by complete disappearance of the intact AP-containing strand and the generation of fast-migrating cleavage products. The slow-migrating product appeared on the gel between the uncross-

linked AP-containing duplex **A** and the "full-size" dG-AP_{red} ICL (duplex **B**). This intermediate gel mobility is consistent with a lower molecular weight cross-link arising from spermine-mediated cleavage of the AP site in duplex **A** (duplex **C** in Figure 1 and Scheme 3).[54, 79-80]

Significantly, no slow-migrating ICL band was generated when the enzyme Endo III was used to induce cleavage of the AP site in duplex **A**. As noted above, the AP lyase activity of Endo III generates the 3'dR cleavage product rather than the α,β-unsaturated 3'PUA product (Scheme 1). Together, the results suggested that cross-link formation arises from an α,β-unsaturated elimination product generated by amine-catalyzed cleavage at the AP site in duplex **A**.

Evidence That the 3'PUA-Iminium Ion Is the Key Intermediate Involved in ICL Formation. Amines catalyze strand cleavage at AP sites via a covalent mechanism involving initial conversion of the AP aldehyde to an iminium ion (Scheme 1).[49, 54-55, 81] The increased acidity of the α-protons in this AP-iminium ion intermediate facilitates β-elimination of the 3'-phosphoryl group.[82-83] The 3'α,β-unsaturated iminium ion (3'PUA-iminium, Scheme 1) is an obligate intermediate in the amine-catalyzed strand cleavage at AP sites in DNA. Importantly, the reactivity of α,β-unsaturated iminium ions is greater than that of the corresponding α,β-unsaturated aldehydes, with respect to the conjugate addition of nucleophiles.[84-86]

With these facts in mind, we examined whether ICL formation induced by spermine-catalyzed cleavage of the AP site in duplex **A** was driven by the 3'PUA-iminium ion, the 3'PUA group, or both. To address this question, we generated the

authentic 3'PUA cleavage product using an established protocol[51] involving heat treatment of the AP-containing duplex. Heating duplex **A** at 95 ˚C for 30 min generated the desired 3'PUA cleavage product in 21% yield, alongside a mixture of the 3'phosphate (24%) cleavage product and the intact AP-containing oligomer (45%, Figure 2, lane 3). Incubation of the duplex containing the 3'PUA cleavage product for 24 h in pH 7.4 buffer at 37 ˚C produced only a trace amount of the slow-migrating ICL band (Figure 2, lane 4). On the other hand, when the AP-containing duplex **A** was heated at 95 ˚C for 30 min, followed by addition of spermine (1 mM) and incubation for 24 h at 37 ˚C, a substantial yield of the slow-migrating ICL band was observed (27%±3, Figure 2, lane 6). Taken together, the results shown in Figures 1 and 2 provided evidence that the 3'PUA group is ineffective at cross-link formation and implicate the 3'PUA-iminium ion as the critical intermediate involved in the spermine-catalyzed generation of an ICL in duplex **A**.

Iron-EDTA-H_2O_2 Footprinting Reveals That the ICL Attachment Is to Opposing Guanine Residues. We employed iron-EDTA footprinting to pinpoint the site(s) of cross-link attachment in the slow-migrating DNA generated by spermine-mediated strand cleavage of the AP-containing duplex **A**. The cross-linked DNA was isolated from a denaturing polyacrylamide gel and subjected to cleavage by an iron-EDTA-H_2O_2 system (Figure S4). In this experiment, the location where the "ladder" of labeled cleavage fragments is interrupted reveals the site of cross-link attachment.[39, 80, 87] The results indicated that the cross-link is attached predominantly (60%) to the guanine residue offset one nucleotide to the 3'-side of the AP site on the opposing strand (the Schemes and Figures illustrate this predominant site of cross-link attachment, see: duplex **C** in Figure 1

and Scheme 3). A significant amount of cross-link (approximately 40%) was attached to the guanine residue directly opposing the AP site.

The footprinting data indicate that the slow-migrating band (lane 7, Figure 1) arising from spermine-mediated cleavage of the AP site in duplex **A** is a *mixture* of two different cross-link attachments. Collectively, the evidence described to this point is consistent with a cross-linking process involving addition of an opposing guanine residue to the α,β-unsaturated iminium ion generated by spermine-mediated strand cleavage at an AP site in duplex DNA (Schemes 3 and 4).

Mass Spectrometric Analysis Is Consistent with Cross-link Formation Involving Conjugate Addition of a Guanine Residue to the 3'PUA-iminium Cleavage Product. The cross-linked DNA generated by spermine-catalyzed strand cleavage of the AP site in duplex **A** was characterized using ESI-QTOF mass spectrometry. The major signal in the deconvoluted mass spectrum corresponded to an *m/z* value of 16081.28 (Figure S5). This value was consistent with a cross-link structure arising from conjugate (aza-Michael-type) addition of an opposing guanine residue to the α,β-unsaturated 3'PUA-iminium ion (calcd *m/z* 16,081.53). We describe this structure as a (3-(2'-deoxyguanosyl)-2,3-dideoxyribose interstrand cross-linkage and use the abbreviation dG-ddR ICL (Schemes 3 and 4).

The dG-ddR ICL Forms Rapidly and Is Chemically Stable Under Physiological Conditions. A formation time-course showed that the cross-linked DNA generated by spermine-mediated cleavage of the AP site in duplex **A** can be detected within minutes

and reaches its half-maximal yield in about 8 h (1 mM spermine, 50 mM HEPES buffer, pH 7.4 containing 100 mM NaCl at 37 ˚C, Figure 3). Formation of this cross-link is substantially faster than other reactions considered to be good candidates for the generation of endogenous ICLs, such as cross-link formation by formaldehyde, acrolein, and 4-hydroxynonenal.[27-29, 88-89] At a longer incubation time (72 h, in the presence of spermine) there is some disappearance of the ICL (Figure 3B). In a separate experiment, cross-linked DNA was isolated by gel electrophoresis and its stability examined in pH 7.4 buffer at 37 ˚C, in the absence of spermine. Under this condition, the cross-link was quite stable, undergoing only about 4% decomposition over the course of 168 h (Figure S6).

The ICL can be decomposed under more vigorous conditions. For example, heating at 95 ˚C in HEPES buffer (50 mM pH 7.4, containing 100 mM NaCl) for 24 h caused disappearance of the cross-linked DNA (Figure S7). Interestingly, treatment of the cross-linked DNA with $NaBH_4$ prior to heating at 95 ˚C dramatically stabilized the material against degradation (Figure S7). Similarly, treatment of the cross-linked DNA with $NaBH_4$ imparted resistance to piperidine-induced disappearance of the cross-linked DNA (1 M, 95 ˚C, 25 min, Figure S7).

The stabilizing effect of $NaBH_4$ is consistent with the structure of the dG-ddR cross-link shown in Scheme 4. Base-mediated decomposition of the ICL is expected to involve β-elimination of the nucleobase initiated by removal of an acidic α-proton from the ring-opened aldehyde form of the cross-link. Reduction of the aldehyde to the corresponding alcohol by $NaBH_4$ will suppress this β-elimination reaction.

A Model Cross-linking Reaction Identifies a Fundamental Preference for Aza-Michael-type Addition of the N^2-Amino Group of 2'-Deoxyguanosine to the α,β-Unsaturated Sugar Remnant. The results described above provided evidence for a previously unknown type of cross-link arising from conjugate addition of a guanine residue to the *trans*-α,β-unsaturated iminium ion produced by amine-catalyzed strand cleavage of the AP site in duplex DNA. However, these results do not rigorously define the exact chemical structure of the cross-link. For example, ICL formation could proceed via addition of the N^2, $N1$, or O^6 atoms of the guanine residue to the 3'PUA-iminium ion intermediate. In addition, reactions with the α,β-unsaturated sugar remnant with the nucleobase can, in principle, proceed via 1,2 (carbonyl) addition, 1,4 (conjugate, Michael-type) addition, or lead to pyrrole formation.[90-91]

To shed light on the chemical structure of the dG-ddR ICL, we designed and characterized a reaction that models this DNA cross-linking process. The model reaction employed (*S*,*E*)-4,5-dihydroxypent-2-enal (**3**) as a mimic of the 3'-*trans*-α,β-unsaturated sugar remnant generated by cleavage of an AP site in DNA.[56-57] This material was prepared by a new route involving periodate oxidation of commercially available 1,2:5,6-di-*O*-isopropylidene-D-mannitol to give the aldehyde **1**, followed by a Wittig condensation with (formylmethylene)triphenylphosphorane to provide the unsaturated aldehyde **2** (Scheme 5, Figure S8). Removal of the acetonide protecting group under acidic conditions gave the desired α,β-unsaturated aldehyde **3** (Scheme 5, Figure S9).

The model cross-linking reaction between the nucleoside 2'-deoxyguanosine and **3** was carried out in a solvent mixture composed of 1:5 DMSO and HEPES buffer (50

mM, pH 7.4) containing arginine as a catalyst.[92-93] Chemical precedents provided by the reactions of 2'-deoxyguanosine with low molecular weight α,β-unsaturated aldehydes enabled us to suspect that this reaction would proceed via aza-Michael-type addition of the exocyclic N^2-amino group of the guanine residue to the α,β-unsaturated sugar residue.[89, 94-95] LC-MS analysis of the reaction revealed a mixture of isomeric products displaying the $[M+H]^+$ ion (at *m*/*z* 384 amu) anticipated for the nucleosidic ICL model **4** (Scheme 5). NMR analyses of this mixture revealed signals consistent with **4**, but detailed assignment of the resonances was not possible due to the complexity of the spectra (up to fourteen equilibrating isomers are possible for this product, four diastereomers of the O-cyclized pyranose form, four diastereomers of the O-cyclized furanose form, four diastereomers of the N-cyclized form, and two enantiomers of the ring-opened form). Treatment of the reaction with $NaBH_4$ (5 equiv) generated a new product mixture **5** that gave dramatically simplified NMR spectra (by removing the possibility for twelve ring-closed isomers). The 1D-NMR, 2D-NMR, and high-resolution mass spectra of this product were consistent with a diastereomeric mixture of the reduced model cross-link **5** (Scheme 5). Key resonances in the 2D-NMR spectra consistent with the connectivity shown for dG-ddR_{red} (**5**) included a correlation between the N^2-H of the guanine residue and the H3" of the 2-deoxyribose adduct in the homonuclear correlation (COSY) spectrum and a correlation between H3" with C2 of the guanine residue and C2" and C1" of the 2-deoxyribose adduct in the heteronuclear multiple bond correlation (HMBC) spectrum (Figure 4 and S10-12).

The results of this model reaction defined a fundamental chemical preference for aza-Michael-type addition of the N^2-amino group of 2'-deoxyguanosine to the α,β-

unsaturated sugar remnant generated by strand cleavage at an AP site in DNA. In addition, the products obtained in this model cross-linking reaction (**4** and **5**, Scheme 5) provided us with structurally-defined standards for use in the LC-MS analyses described in the next section.

LC-MS/MS/MS Analyses Define the Structure of the dG-ddR ICL Generated in Duplex DNA. The cross-linked DNA generated by spermine-mediated cleavage of the AP-containing duplex **A** was isolated and digested using a four-enzyme cocktail consisting of nuclease P1, alkaline phosphatase, and phosphodiesterases I and II. We analyzed cross-linked DNA both with and without $NaBH_4$ treatment. Selected-ion chromatograms from the LC-MS/MS analysis of the digests were obtained using previously reported conditions.[96-98]

Analysis of the cross-linked DNA that was treated with $NaBH_4$ revealed two peaks eluting at 16.9 and 18.2 min displaying the *m/z* 386→270 transition anticipated for the neutral loss of 2-deoxyribose from the dG-ddR_{red} cross-link remnant (Figure 5A). Further cleavage of the *m/z* 270 ion produced a fragment ion at *m/z* 152 in MS/MS/MS, corresponding to the $[M+H]^+$ ion of the free guanine base (Figure S13).

The chemical model reaction described in the previous section provided a structurally-defined standard for comparison against the actual ICL remnant obtained by digestion of cross-linked DNA. We found that the LC-MS properties of the synthetic standard **5** (Figure 5B) mirrored those of the actual cross-link remnant obtained by enzymatic digestion of the cross-linked, $NaBH_4$-treated DNA (Figure 5A). The multiple peaks displaying the *m/z* 386→270 transition in the LC-MS/MS ion chromatograms

presumably reflect diastereomers generated in the conjugate addition reaction (in both the model reaction and the actual DNA cross-linking reaction). Additional LC-MS/MS/MS analyses (Figure S13) of the unreduced cross-link were consistent with the dG-ddR cross-link structures depicted in Schemes 3, 4, and 5.

Overall, the LC-MS analyses utilizing structurally-characterized synthetic standards enabled us to establish the chemical structure of the ICL formed by spermine-mediated strand cleavage in duplex **A** (dG-ddR, Scheme 4). In addition, the LC-MS workflow described here provides a platform that may be used for the detection of this novel ICL in cellular DNA.

The dG-ddR Cross-Link Blocks DNA Replication by the Highly Processive, Strand-Displacing ϕ29 Polymerase. The dG-ddR cross-link is nominally reversible via a retro-aza-Michael reaction.[99] Nonetheless, the results shown above indicate that the dG-ddR ICL possesses substantial chemical stability in duplex DNA (Figures 3 and S6). However, from a biological perspective, it may be most important to determine whether the cross-link can block the action of proteins that actively induce strand separation during DNA replication and transcription.[100] To explore this issue, we examined the ability of the bacteriophage ϕ29 DNA polymerase to carry out strand-displacement synthesis on templates containing the dG-ddR ICL. This enzyme has been described as a hybrid polymerase-helicase that actively unwinds duplex DNA while simultaneously carrying out highly processive DNA synthesis.[101]

First, we confirmed that the ϕ29 polymerase fully extended a primer on a single-stranded template or on templates containing regions of duplex DNA in the path of the

polymerase (Figure S14). In contrast, conjugation of a complementary strand to the template via the dG-ddR ICL blocked primer extension by the polymerase (Figure 6 and S14). Primer extension stalled at the last unmodified nucleotides prior to the site of cross-link attachment (Figure 6). A template containing the "full-sized" dG-AP_{red} cross-link previously shown to block primer extension by ϕ29 was employed as a comparison (Figure 6).[102]

A group of previous studies showed that the ability to block primer extension by ϕ29 polymerase in vitro is predictive of ICL properties in biological systems. Specifically, the ability of the dA-AP ICL to stall primer extension by ϕ29 accurately forecasted the ability of this ICL to block DNA replication in a eukaryotic cell extract.[26, 102-103] Accordingly, the results reported here suggest that the dG-ddR ICL has the capacity to block critical cellular DNA transactions that require strand separation.

Unhooking of the dG-ddR ICL by Human Apurinic/apyrimidinic Endonuclease 1 (hAPE1). We next considered whether this structurally-novel ICL might be subject to repair by a novel mechanism. Specifically, we explored whether the enzyme apurinic endonuclease 1 (APE1) has the potential to initiate repair of the dG-ddR ICL. APE1 plays a central role in the base excision repair (BER) pathway.[104] In this capacity, the endonuclease activity of APE1 hydrolyzes the phosphodiester linkage on the 5'-side of AP sites that are generated when damaged or mispaired bases are removed by BER glycosylases.[105] This reaction generates a one-nucleotide gap with 3'OH and 5'deoxyribose phosphate termini.

APE1 also has a distinct 3'-exonuclease activity that enables the removal of mismatched nucleotides and sugar remnants from the 3'-terminus of strand breaks. This activity is important in BER and single-strand break repair (SSBR) pathways.[59, 63, 104-107] Recent structural studies revealed that the 3'-exonuclease activity of hAPE1 does not require extrusion ("flipping") of the mispaired nucleotide from a gapped duplex.[104, 106, 108] This structural data suggested to us that the dG-ddR ICL might be a competent substrate for the 3'-exonuclease activity of APE1. Importantly, 3'-exonuclease activity of APE1 on the dG-ddR ICL would serve to "unhook" the cross-link, perhaps initiating repair through a variant of the single-strand break repair (SSBR) pathway (Schemes 3 and 6).[32]

We found that the dG-ddR ICL in DNA was, indeed, unhooked by APE1 (Figure 7). A time course of this reaction showed that unhooking occurs with a half-time of 10-15 min. The gel mobility of the initial unhooked product was consistent with the 3'OH end group expected for the 3'-exonuclease activity of the enzyme. At longer incubation times, smaller oligodeoxynucleotide products arising from further 3'-exonuclease activity of APE1 on the initial unhooking product were observed (Figure 7).[109]

APE1 was more effective at unhooking the dG-ddR ICL in a "gapped" substrate (Figure 7) than in a resected (3'-recessed) substrate lacking the oligonucleotide fragment on the 3'-side of the strand break (Figure S15). This mirrors the preference reported for the 3'-exonuclease activity of APE1 on mispaired 3'-nucleotides.[107] In addition, unhooking of the dG-ddR ICL by APE1 was more effective when carried out in a buffer optimized[110] for the 3'-exonuclease activity of the enzyme rather than the typical buffer optimized for endonuclease activity (Figure S16). The unhooking reactions do not proceed to completion. Likely this reflects product inhibition of the enzyme (Figure

S16). APE1 is inhibited by the 5'-incised product generated by the endonuclease action on an AP site in duplex DNA and binds a variety of incised, gapped, nicked and 3'-recessed duplexes (Figure S16).

For comparison, we characterized the ability of APE1 to trim the 3'dR end group generated by the action of *E. coli* Endo III on the AP site in duplex **A**. Sugar remnants derived from the AP-lyase activity of BER glycosylases are known substrates for the 3'-exonuclease activity of APE1.[59, 61, 63, 104-107] Removal of the 3'dR end group from a gapped substrate by APE1 (1 unit/μL) took place with a half-time of approximately 5-10 min (Figure S17). The unhooking of the dG-ddR ICL by APE1 described above was somewhat less effective than the trimming of the 3'dR end group, requiring 2-fold greater enzyme concentration to proceed at a comparable rate.

Finally, we examined whether the lyase activity associated with BER glycosylases can unhook the dG-ddR ICL. In principle, unhooking of the dG-ddR ICL via a retro aza-Michael mechanism might be catalyzed by enzymes with amine-dependent AP-lyase activity. However, we found that the base excision repair glycosylase FPG, an enzyme with very effective lyase activity,[111] did not unhook the dG-ddR ICL (Figure S18).

Scope and Generality of the Cross-Linking Reaction: Formation of the dG-ddR ICL In Various Sequences and Under Varied Conditions. To examine the scope and generality of this new DNA cross-linking process we measured spermine-induced ICL formation in a series of AP-containing duplex sequences containing single guanine residues located on the opposing strand near the strand cleavage site (Figure 8). We

found that spermine-induced cleavage of the AP site in all these duplexes led to the generation of slow-migrating ICL bands (Figure 8). Among the three "single-G" sequences, the highest ICL yield was obtained in the duplex containing a guanine residue offset one nucleotide to the 3'-side of the AP site on the opposing strand. The major signal observed in the mass spectrometric analysis of the cross-linked DNA generated in this sequence was consistent with that expected for the dG-ddR ICL attachment (Figure S19). The trends in the ICL yields observed for the single-G duplexes mirrored the preferred cross-link locations in the triple-G sequence of duplex **A**.

We examined spermine-mediated ICL formation in the AP-containing duplexes **D** and **G** each containing the same triple-G core cross-linking site found in duplex **A**, but with differing numbers of base pairs on the 3'-side of the AP site (7, 17, and 27 bp, Figure S20). There are significant differences in the architecture of the products generated by strand cleavage of the AP site in these duplexes. Specifically, following cleavage at the AP site in duplex **D**, the 7 nt fragment will "melt off" to yield a 3'-recessed (resected) cleavage site. On the other hand, the 17 and 27 nt fragments generated by cleavage at the AP site in duplexes **A** and **G** will remain hybridized to give gapped cleavage sites. We observed substantial yields of cross-link in all of these duplexes, with the ICL yields following the trend of **D** > **A** > **G**. The results suggest that the dG-ddR ICL can form at both gapped and resected (3'-recessed) strand cleavage sites (Figure S20).

We examined the DNA cross-linking reaction in different buffers. Our standard cross-linking conditions involved incubation of the AP-containing duplex **A** with spermine (1 mM) in HEPES buffer (50 mM, pH 7.4) containing NaCl (100 mM) for 24 h

at 37 ˚C to give a 31±3% yield of the ICL (Figure 1). We observed significant amounts of ICL generated by spermine-induced cleavage of the AP site in duplex **A** in Tris-HCl (50 mM, pH 7.4, containing 100 mM NaCl, 19±2% yield) and sodium phosphate (50 mM, pH 7.4, containing 100 mM NaCl, 38±2% yield, Figure S21) after incubation for 24 h at 37 ˚C. Spermine-induced strand cleavage of duplex **A** in sodium acetate (750 mM, pH 5.2) at 37 ˚C for 24 h gave a low yield of the slow-migrating ICL band (3±1%). No significant yields of ICL were observed under any of these conditions in the absence of spermine.

Finally, we examined the ability of amines other than spermine to induce ICL formation in HEPES buffer (50 mM, pH 7.4 containing 100 mM NaCl at 37 ˚C, for 24 h). We found that *N*,*N*'-dimethylethylenediamine (1 mM),[53] the Lys-Trp-Lys tripeptide (100 μM)[55, 57, 112] and putrescine (1 mM)[53] induced ICL formation in yields of, 4%, 3%, and 1%, respectively. The ICL yields induced by these amines were substantially less than that generated by spermine. Arginine and lysine (1 mM) did not induce significant amounts of the ICL.

It is interesting to consider the mechanistic reasons for these results. Arginine, lysine, and putrescine do not induce induce ICL formation because they do not significant amounts of strand cleavage at the AP site (Figure S21). Strand cleavage by *N*,*N*'-dimethylethylenediamine is slow relative to spermine, with significant amounts of uncleaved AP site still present after 24 h (Figure S21). Lys-Trp-Lys effectively induces strand cleavage but forms a stable adduct with the cleavage product that evidently inhibits ICL formation (Figure S21). Spermine is particularly effective at catalyzing cleavage of AP sites because, in neutral aqueous solution, one of its four amine residues

(unlike most amines) presents substantial amounts of the nucleophilic free base required for reaction with the AP aldehyde in the first step of iminium ion formation.[53]

Overall, the results indicate that formation of the dG-ddR ICL arising from spermine-catalyzed cleavage of AP sites in duplex DNA can be formed in a wide variety of buffers and in diverse sequence environments.

CONCLUSIONS

Amine-catalyzed β-elimination of the 3'-phosphoryl group from an AP site unmasks a latent electrophile in the midst of a nicked DNA duplex. We characterized a structurally novel ICL lesion arising from aza-Michael-type addition of the exocyclic N^2-amino group of a guanine residue to the α,β-unsaturated sugar remnant generated by amine catalyzed strand cleavage at an AP site in duplex DNA. Our evidence suggests that the α,β-unsaturated iminium ion intermediate is directly involved in the cross-linking reaction (3'PUA-iminium ion, Schemes 1 and 4). In contrast, the α,β-unsaturated aldehyde (3'PUA, Scheme 1) was ineffective at cross-link generation under our reaction conditions. This process yields a complex clustered lesion consisting of a cross-link coupled to a single-strand break.

AP sites that serve as the precursor to the dG-ddR ICL are common in cellular DNA.[33-35] Likewise, spermine and related polyamines are abundant in cells.[52, 73-76] Accordingly, this ICL can be added to the list of potential endogenous ICLs in cellular DNA.[27] To date, there is little information regarding the identity and levels of ICLs in the DNA of living cells.[27] The detection of endogenous ICLs in living systems inevitably presents significant challenges because cells are not likely to tolerate more than low

levels of these replication- and transcription-blocking lesions. Nonetheless, the LC-MS experiments described here provide a platform for future studies aimed at detection of this ICL in cellular DNA.

Endogenous ICLs that block replication and transcription have the potential to contribute to cancer, neurodegeneration, and aging.[16, 28, 30-31] Our results show that the dG-ddR ICL blocks DNA replication by the highly processive, strand-separating ϕ29 DNA polymerase, even under forcing conditions employing high dNTP concentrations and long incubation times. This suggests that, owing to their ability to block critical cellular DNA transactions that require strand separation, unrepaired dG-ddR cross-links have the potential to have significant biological consequences stemming from their ability to induce cell death, senescence, and dysfunction.

It is interesting to speculate on processes by which this novel ICL might be removed from cellular DNA. The DNA repair protein PARP1 recognizes single-strand breaks in DNA.[32, 113] Accordingly, recognition of the dG-ddR strand break/ICL by PARP1 may recruit XPC, ultimately leading to unhooking of the ICL via a 5'-incision carried out by the nucleotide excision repair (NER) proteins XPF-ERCC1.[114] With respect to NER, it is important to recognize that previous studies with architecturally similar ICLs[79-80] derived from strand cleavage at oxidized AP sites suggest that dysregulated generation of incisions has the potential to convert strand-break/ICLs into toxic double-strand breaks.[115-116] Based on this precedent, the possibility for dysfunctional NER presumably exists for the dG-ddR strand-break-ICL described here. However, our biochemical experiments offer an alternative possibility that this type of

structurally complex ICL might be repaired by a surprisingly simple mechanism in which the cross-link is unhooked by the enzyme APE1.

The enzyme APE1 is best known for its ability to incise duplex DNA on the 5'-side of AP sites generated spontaneously or by DNA glycosylases during BER.[104-105] In addition, APE1 has a 3'-exonuclease activity that may play an important role in removing sugar remnants from the 3'-terminus of strand breaks generated by oxidative DNA damage, BER, or spontaneous cleavage at AP sites.[32, 63, 104-107, 109-110, 117] Other enzymes including tyrosyl phosphodiesterases (TDP) and APE2 similarly participate in 3'end-cleaning.[118-120] The removal of 3'-blocking groups from strand breaks is critical to reveal the 3'OH group required for completion of DNA repair and replication.[58-59, 120]

We find that the 3'-exonuclease activity of APE1 unhooks the dG-ddR ICL. This unprecedented ICL unhooking activity of APE1 has the capacity to initiate repair of the cross-link through a variant of the single-strand break repair pathway (SSBR). The canonical SSBR pathway can be viewed as a sub-pathway of base excision repair (BER) involving recognition of the single-strand break, enzymatic trimming of 2-deoxyribose sugar remnants ("dirty ends") from the 5' or 3' termini of the break, gap-filling by polymerase β, and sealing of the nicked duplex by a DNA ligase.[32, 105, 117] The protein PARP1 may be involved in sensing the strand break[32, 113] and the protein XRCC1 acts as a scaffold to organize this multi-protein complex on DNA.[32, 105, 117, 121]

The gapped duplex generated by the 3'-exonuclease action of APE1 on the dG-ddR ICL closely resembles a typical SSBR substrate, with the exception that a guanine residue on the template strand opposing the break bears an N^2-deoxyribosyl-5-phosphate (dRP) adduct (Scheme 6). The residual N^2-dRP adduct may be subject to error-prone or

error-free replication involving translesion bypass polymerases such as pol κ, ι, and ζ.[122] Alternatively, the N^2-dRP adduct could be removed during SSBR by an atypical dRP lyase activity of pol β[123] or excised after SSBR by NER.[124]

In summary, we characterized a previously unknown, structurally complex cross-link arising from a common endogenous lesion in DNA. Our biochemical studies suggest that this ICL has the potential to block critical DNA transactions such as replication and transcription, but also offer the possibility that this complex lesion may be removed from genomic DNA by a remarkably simple process in which unhooking of the cross-link by APE1 channels repair through a variant of the SSBR pathway, thereby evading complex classical ICL repair pathways and the potential for dysfunctional NER repair.

■ ASSOCIATED CONTENT

Supporting Information

The Supporting Information is available free of charge via the Internet at http://pubs.acs.org.

Additional information including sequences used, characterization of Endo III cleavage products, detail on dG-AP ICL, ICL footprinting, ESI-TOF MS analysis of cross-linked DNA, stability of ICL, effects of $NaBH_4$ treatment on cross-link stability, NMR structure elucidation of the model cross-link **5**, LC-MS data, polymerase blocking data, APE1 unhooking data, and treatment of cross-linked duplex with FPG, cross-link formation in duplexes with single opposing guanine residues, cross-link formation in gapped and resected duplexes, and ICL formation induced by amines other than spermine.

■ AUTHOR INFORMATION

Corresponding Authors

Kent S. Gates – Departments of Chemistry and Biochemistry, 125 Chemistry Bldg. University of Missouri, Columbia, MO 65211, United States; ORCHID ID: 0000-0002-4218-7411; Phone: (573) 882-6763; Email: gatesk@missouri.edu

Authors

Kurt Housh – Department of Chemistry, 125 Chemistry Bldg, University of Missouri, Columbia, MO 65211, United States

Jay S. Jha – Department of Chemistry, 125 Chemistry Bldg, University of Missouri, Columbia, MO 65211, United States

Zhiyu Yang – Department of Chemistry, 125 Chemistry Bldg, University of Missouri, Columbia, MO 65211, United States

Tuhin Haldar – Department of Chemistry, 125 Chemistry Bldg, University of Missouri, Columbia, MO 65211, United States

Kevin M. Johnson – Department of Chemistry, 125 Chemistry Bldg, University of Missouri, Columbia, MO 65211, United States

Jiekai Yin – Department of Chemistry, University of California Riverside, Riverside, CA 92521-0403, United States

Yinsheng Wang – Department of Chemistry, University of California Riverside, Riverside, CA 92521-0403, United States; ORCHID ID: 0000-0001-5565-283X; Phone (951) 827-2700; Email: yinsheng@ucr.edu

Notes.

The authors declare no conflicts of interest

■ ACKNOWLEDGEMENTS

We are grateful to the National Institutes of Health for support of this work (ES021007 to KSG and YW). We thank Deepak Ahire for preliminary experiments related to synthesis of the dG-ddR model ICL.

■ REFERENCES

1. Crick, F. H. C., Central dogma of molecular biology. *Nature* **1970,** *227* (5258), 561-563.
2. Callaway, E., Mammoth genomes shatter the record for oldest ancient DNA. *Nature* **2021,** *590*, 537-538.
3. Allentoft, M. E.; Collins, M.; Harker, D.; Haile, J.; Oskam, C. L.; Hale, M. L.; Campos, P. F.; Samaniego, J. A.; Gilbert, M. T. P.; Willerslev, E.; Zhang, G.; Scofield, R. P.; Holdaway, R. N.; Bunce, M., The half-life of DNA in bone: measuring decay kinetics in 158 dated fossils. *Proc. R. Soc. B* **2012,** *279*, 4724–4733.
4. Church, G. M.; Gao, Y.; Kosuri, S., Next generation information storage in DNA. *Science* **2012,** *337*, 1628.
5. Matange, K.; Tuck, J. M.; Keung, A. J., DNA stability: a central design consideration for DNA data storage systems. *Nat Commun* **2021,** *12* (1), 1358.
6. Fekry, M. I.; Tipton, P. A.; Gates, K. S., Kinetic consequences of replacing the internucleotide phosphorus atoms in DNA with arsenic. *ACS Chem Biol* **2011,** *6* (2), 127-30.

7. Frederico, L. A.; Kunkel, T. A.; Shaw, B. R., A sensitive genetic asssay for detection of cytosine deamination: determination of rate constants and the activation energy. *Biochemistry* **1990,** *29* (10), 2532-2537.
8. Lindahl, T.; Nyberg, B., Rate of depurination of native deoxyribonucleic acid. *Biochemistry* **1972,** *11* (19), 3610-3618.
9. Gates, K. S., An overview of chemical processes that damage cellular DNA: spontaneous hydrolysis, alkylation, and reactions with radicals. *Chem. Res. Toxicol.* **2009,** *22* (11), 1747-1760.
10. Lander, E. S., Initial impact of the sequencing of the human genome. *Nature* **2011,** *470* (7333), 187-197.
11. Gates, K. S.; Nooner, T.; Dutta, S., Biologically relevant chemical reactions of N7-alkyl-2'-deoxyguanosine adducts in DNA. *Chem. Res. Toxicol.* **2004,** *17* (7), 839-856.
12. Lindahl, T.; Ljunquist, S.; Siegert, W.; Nyberg, B.; Sperens, B., DNA N-glycosidases: properties of uracil-DNA glycosidase from Escherichia coli. . *J. Biol. Chem.* **1977,** *252*, 3286-3294.
13. Guillet, M.; Bioteux, S., Origin of endogenous DNA abasic sites in Saccaromyces cerevisiae. *Mol. Cell Biol.* **2003,** *23* (22), 8386-8394.
14. Roberts, S. A.; Lawrence, M. S.; Klimczak, L. J.; Grimm, S. A.; Fargo, D.; Stojanov, P.; Kiezun, A.; Kryukov, G. V.; Carter, S. L.; Saksena, G.; Harris, S.; Shah, R. R.; Resnick, M. A.; Getz, G.; Gordenin, D. A., An APOBEC cytidine deaminase mutagenesis pattern is widespread in human cancers. *Nature Genet.* **2013,** *45*, 970-976.
15. Tubbs, A.; Nussenszweig, A., Endogenous DNA Damage as a Source of Genomic Instability in Cancer. *Cell* **2017,** *168*, 644-656.
16. Yousefzadeh, M.; Henpita, C.; Vyas, R.; Soto-Palma, C.; Robbins, P. N., L. , DNA damage-how and why we age? *eLife* **2021,** *10*, e62852.
17. Friedberg, E. C.; McDaniel, L. D.; Schultz, R. A., The role of endogenous and exogenous DNA damage and mutagenesis. *Curr. Opin. Genetics Devel.* **2004,** *14*, 5-10.
18. Hershberg, R., Mutation—The Engine of Evolution: Studying Mutation and Its Role in the Evolution of Bacteria. *Cold Spring Harb. Perspect. Biol.* **2015,** *7* (9), a018077.
19. Lodato, M. A.; Rodin, R. E.; Bohrson, C. L.; Coulter, M. E.; Barton, A. R.; Kwon, M.; Sherman, M. A.; Vitzthum, C. A.; Luquette, L. J.; Yandava, C. N.; Yang, P.; Chittenden, T. W.; Hatem, N. E.; Ryu, S. C.; Woodworth, M. B.; Park, P. J.; Walsh, C. A., Aging and neurodegeneration are associated with increased mutations in single human neurons. *Science* **2018,** *359*, 555-559.
20. Lindahl, T., The Intrinsic Fragility of DNA (Nobel Lecture). *Angew. Chem. Int. Ed. Eng.* **2016,** *55*, 8528 –8534.
21. Groth, V. D.; Carlsson, R.; Johansson, F.; Erixon, K.; Jenssen, D., DNA interstrand crosslinks induce a potent replication block followed by formation and repair of double strand breaks in intact mammalian cells. *DNA Repair* **2012,** *11* (12), 976-985.
22. Derheimer, F. A.; Hicks, J. K.; Paulsen, M. T.; Canman, C. E.; Ljungman, M., Psoralen-induced DNA interstrand cross-links block transcription and induce p53 in an ataxia-telangiectasia and rad3-related-dependent manner. *Mol. Pharm.* **2009,** *75* (3), 599-607.
23. Williams, H. L.; Gottesman, M. E.; Gautier, J., The differences between ICL repair during and outside of S phase. *Trends Biochem. Sci* **2013,** *38* (8), 386-393.

24. Clauson, C.; Schärer, O. D.; Niedernhofer, L. J., Advances in understanding the complex mechanisms of DNA interstrand cross-link repair. *Cold Spring Harbor Perspectives in Biology* **2013,** *5* (10), a012732/1-a012732/25.
25. Wu, R. A.; Semlow, D. R.; Kamimae-Lanning, A. N.; Kochenova, O. V.; Chistol, G.; Hodskinson, M. R. G.; Amunugama, R.; Sparks, J. L.; Wang, M.; Deng, L.; Mimoso, C. A.; Low, E.; Patel, K. J.; Walter, J. C., TRAIP is a master regulator of DNA interstrand crosslink repair. *Nature* **2019,** *567-272*.
26. Yang, Z.; Nejad, M. I.; Gamboa Varela, J.; Price, N. E.; Wang, Y.; Gates, K. S., A role for the base excision repair enzyme NEIL3 in replication-dependent repair of interstrand cross-links derived from psoralen and abasic sites. *DNA Repair* **2017,** *52*, 1-11.
27. Housh, K.; Jha, J. S.; Haldar, T.; Binth Md. Amin, S.; Islam, T.; Wallace, A.; Gomina, A.; Guo, X.; Nel, C.; Wyatt, J. W.; Gates, K. S., Formation and repair of unavoidable, endogenous interstrand cross-links in cellular DNA. *DNA Repair* **2021,** *98*, 103029.
28. Duxin, J. P.; Walter, J. C., What is the DNA repair defect underlying Fanconi anemia. *Curr. Opin. Cell. Biol.* **2015,** *37*, 49-60.
29. Sakai, W.; Sugasawa, K., Importance of finding the bona fide target of the Fanconi anemia pathway. *Genes Environ.* **2019,** *41* (6), doi.org/10.1186/s41021-019-0122-y.
30. Tiwari, V.; Wilson III, D. M., DNA damage and associated DNA repair defects in disease and premature aging. *Am. J. Hum. Genet.* **2019,** *105*, 237-257.
31. O'Driscoll, M., Diseases Associated with Defective Responses to DNA Damage. *Cold Spring Harb. Perspect. Biol.* **2012,** *4*, a012773.
32. Abbotts, R.; Wilson III, D. M., Coordination of single strand break repair. *Free Rad. Biol. Med.* **2017,** *107*, 228-244.
33. De Bont, R.; van Larebeke, N., Endogenous DNA damage in humans: a review of quantitative data. *Mutagenesis* **2004,** *19* (3), 169-185.
34. Swenberg, J. A.; Moeller, B. C.; Gao, L.; Upton, P. B.; Nakamura, J.; Starr, T., Endogenous versus exogenous DNA adducts: their role in carginogenesis, epidemiology, and risk assessment. *Toxicol. Sci.* **2011,** *120* (S1), S130-S145.
35. Chen, H.; Yao, L.; Brown, C.; Rizzo, C. J.; Turesky, R. J., Quantitation of Apurinic/Apyrimidinic Sites in Isolated DNA and in Mammalian Tissue with a Reduced Level of Artifacts. *Anal. Chem.* **2019**, 7403-7410.
36. Wilde, J. A.; Bolton, P. H.; Mazumdar, A.; Manoharan, M.; Gerlt, J. A., Characterization of the equilibrating forms of the abasic site in duplex DNA using 17O-NMR. *J. Am. Chem. Soc.* **1989,** *111*, 1894-1896.
37. Imani-Nejad, M.; Price, N. E.; Haldar, T.; Lewis, C.; Wang, Y.; Gates, K. S., Interstrand DNA cross-links derived from reaction of a 2-aminopurine residue with an abasic site. *ACS Chem. Biol.* **2019,** *14* (1481-1489).
38. Gamboa Varela, J.; Gates, K. S., A Simple, High-Yield Synthesis of DNA Duplexes Containing a Covalent, Thermally-Reversible Interstrand Cross-link At a Defined Location *Angew. Chem. Int. Ed. Eng.* **2015,** *54*, 7666-7669.
39. Johnson, K. M.; Price, N. E.; Wang, J.; Fekry, M. I.; Dutta, S.; Seiner, D. R.; Wang, Y.; Gates, K. S., On the Formation and Properties of Interstrand DNA-DNA

Cross-links Forged by Reaction of an Abasic Site With the Opposing Guanine Residue of 5'-CAp Sequences in Duplex DNA. *J. Am. Chem. Soc.* **2013,** *135*, 1015-1025.
40. Price, N. E.; Johnson, K. M.; Wang, J.; Fekry, M., I.; Wang, Y.; Gates, K. S., Interstrand DNA−DNA Cross-Link Formation Between Adenine Residues and Abasic Sites in Duplex DNA. *J. Am. Chem. Soc.* **2014,** *136*, 3483−3490.
41. Catalano, M. J.; Price, N. E.; Gates, K. S., Effective molarity in a nucleic acid controlled reaction. *Bioorg. Med. Chem. Lett.* **2016,** *26* (11), 2627–2630.
42. Thompson, P. S.; Amidon, K. M.; Mohni, K. N.; Cortez, D.; Eichman, B. F., Protection of abasic sites during DNA replication by a stable thiazolidine protein-DNA cross-link. *Nature Struct. Mol. Biol.* **2019,** *26*, 613-618.
43. Ren, M.; Shang, M.; Wang, H.; Xi, Z.; Zhou, C., Histones participate in base excision repair of 8-oxodGuo by transiently cross-linking with active repair intermediates in nucleosome core particles. *Nucleic Acids Res.* **2021,** *49*, 257-268.
44. Dutta, S.; Chowdhury, G.; Gates, K. S., Interstrand crosslinks generated by abasic sites in duplex DNA. *J. Am. Chem. Soc.* **2007,** *129*, 1852-1853.
45. Imani-Nejad, M.; Guo, X.; Housh, K.; Nel, C.; Yang, Z.; Price, N. E.; Wang, Y.; Gates, K. S., Preparation and purification of oligodeoxynucleotide duplexes containing a site-specific, reduced, chemically stable covalent interstrand cross-link between a guanine residue and an abasic site. *Methods Mol. Biol.* **2019,** *1973* (Non-natural Nucleic Acids), 163-175.
46. Guthrie, J. P.; Cossar, J.; Klym, A., Halogenation of acetone. A method for determining pKas of ketones in aqueous solution, with an examination of the thermodynamics and kinetics of alkaline halogenation and a discussion of the best value for the rate constant for a diffusion-controlled reaction. Energetic requirements for a diffusion-controlled reaction involving heavy-atom bond formation. *J. Am. Chem. Soc.* **1984,** *106* (5), 1351–1360.
47. Rahimoff, R.; Kosmatchev, O.; Kirchner, A.; Pfaffeneder, j.; Spada, F.; Brantl, V.; Müller, M.; Carell, T., 5-Formyl- and 5-carboxydeoxycytidines do not cause accumulation of harmful repair intermediates in stem cells. *J. Am. Chem. Soc.* **2017,** *139*, 10359-10364.
48. Lindahl, T.; Andersson, A., Rate of chain breakage at apurinic sites in double-stranded deoxyribonucleic acid. *Biochemistry* **1972,** *11*, 3618-3623.
49. Bailly, V.; Verly, W. G., Escherichia coli endonuclease III is not an endonuclease but a beta-elimination catalyst. *Biochem. J.* **1987,** *242*, 565-572.
50. Zhou, C.; Sczepanski, J. T.; Greenberg, M. M., Mechanistic studies on histone catalyzed cleavage of apyrimidinic/apurinic sites in nucleosome core particles. *J. Am. Chem. Soc.* **2012,** *134*, 16734-16741.
51. Sugiyama, H.; Fujiwara, T.; Ura, A.; Tashiro, T.; Yamamoto, K.; Kawanishi, S.; Saito, I., Chemistry of thermal degradation of abasic sites in DNA. mechanistic investigation on thermal DNA strand cleavage of alkylated DNA. *Chem. Res. Toxicol.* **1994,** *7*, 673-683.
52. Male, R.; Fosse, V. M.; Kleppe, K., Polyamine-induced hydrolysis of apurinic sites in DNA and nucleosomes. *Nucleic Acid Res.* **1982,** *10* (20), 6305-6318.
53. McHugh, P. J.; Knowland, J., Novel reagents for chemical cleavage at abasic sites and UV photoproducts in DNA. *Nucleic Acids Res.* **1995,** *23* (10), 1664-1670.

54. Yang, Z.; Price, N. E.; Johnson, K. M.; Wang, Y.; Gates, K. S., Interstrand cross-links arising from strand breaks at true abasic sites in duplex DNA. *Nucleic Acids Res.* **2017,** *45*, 6275-6283.
55. Kurtz, A. J.; Dodson, M. L.; Lloyd, R. S., Evidence for multiple imino intermediates and identification of reactive nucleophiles in peptide-catalyzed beta-elimination at abasic sites. *Biochemistry* **2002,** *41*, 7054-7064.
56. Mazumdar, A.; Gerlt, J. A.; Rabow, L.; Absalon, M. J.; Stubbe, J.; Bolton, P. H., UV endonuclease V from bacteriophage T4 catalyzes DNA strand cleavage at aldehydic abasic sites by a syn beta-elimination reaction. *J. Am. Chem. Soc.* **1989,** *111*, 8029-8030.
57. Mazumder, A.; Gerlt, J. A.; Absalon, M. J.; Stubbe, J.; Cunningham, R. P.; Withka, J.; Bolton, P. H., Stereochemical studies of the b-elimination reactions at aldehydic abasic sites in DNA: endonuclease III from Escherichia coli, sodium hydroxide, and Lys-Trp-Lys. *Biochemistry* **1991,** *30* (4), 1119-26.
58. Shen, B.; Chapman, J. H.; Custance, M. F.; Tricola, G. M.; Jones, C. E.; Furano, A. V., Perturbation of base excision repair sensitizes breast cancer cells to APOBEC3 deaminase-mediated mutations. *Elife* **2020,** *9*.
59. Maher, R. L.; Wallace, S. S.; Pederson, D. S., The lyase activity of bifunctional DNA glycosylases and the 3'-phosphodiesterase activity of APE1 contribute to the repair of oxidized bases in nucleosomes. *Nucleic Acids Res.* **2019,** *47* (6), 2922-2931.
60. O'Brien, P. J.; Siraki, A. G.; Shangari, N., Aldehyde sources, metabolism, molecular toxicity, and possible effects on human health. *Crit. Rev. Toxicol.* **2005,** *35*, 609-662.
61. Wiederhold, L.; Leppard, J. B.; Kedar, P.; Karimi-Busheri, F.; Rasouli-Nia, A.; Weinfeld, M.; Tomkinson, A. E.; Izumi, T.; Prasad, R.; Wilson, S. H.; Mitra, S.; Hazra, T. K., AP endonuclease-independent DNA base excision repair in human cells. *Mol. Cell* **2004,** *15*, 209-220.
62. Levin, J. D.; Johnson, A. W.; Demple, B., Homogeneous Escherichia coli endonuclease IV. Characterization of an enzyme that recognizes oxidative damage in DNA. *J. Biol. Chem.* **1988,** *263* (17), 8066-8071.
63. Wilson III, D. M., Processing of nonconventional DNA strand break ends. *Env. Mol. Mutagenesis* **2007,** *48*, 772-782.
64. Varshney, U.; van de Sande, J. H., Specificities and kinetics of uracil excision from uracil-containing DNA oligomers by Escherichia coli uracil DNA glycosylase. *Biochemistry* **1991,** *30*, 4055-4061.
65. Stuart, G. R.; Chambers, R. W., Synthesis and properties of oligodeoxynucleotides with an AP site at a preselected position. *Nucleic Acids Res.* **1987,** *15* (18), 7451-7462.
66. Alexeeva, M.; Moen, M. N.; Grosvik, K.; Tesfahun, A. N.; Xu, X. M.; Muruzabal-Lecumberri, I.; Olsen, K. M.; Rasmussen, A.; Ruoff, P.; Kirpekar, F.; Klungland, A.; Bjelland, S., Excision of uracil from DNA by hSMUG1 includes strand incision and processing. *Nucleic Acids Res* **2019,** *47* (2), 779-793.
67. Bailly, V.; Derydt, M.; Verly, W. G., gamma-Elimination in the repair of AP (apurinic/apyrimidinic) sites in DNA. *Biochem. J.* **1989,** *261*, 707-713.
68. Mattes, W. B.; Hartley, J. A.; Kohn, K. W., Mechanism of DNA strand breakage by piperidine at sites of N7 alkylation. *Biochim. Biophys. Acta* **1986,** *868*, 71-76.

69. Maxam, A. M.; Gilbert, W., Sequencing end-labeled DNA with base-specific chemical cleavages. *Methods Enzymol.* **1980,** *65*, 499-560.
70. New England Biolabs Catalog 2019-20. https://www.neb.com/products/m0268-endonuclease-iii-nth#Product%20Information (accessed 2021-08-30), pp 107 and 109.
71. D'Ham, C.; Romieu, A.; Jaquinod, M.; Gaparutto, D.; Cadet, J., Excision of 5,6-dihydroxy-5,6-dihydrothymine, 5,6-dihydrothyine, and 5-hydroxycytosine from define sequence oligonucleotides by Escherichia coli endonuclease III and Fpg proteins: Kinetic and mechanistic aspects. *Biochemistry* **1999,** *38*, 3335-3344.
72. Darwanto, A.; Farrel, A.; Rogstad, D. K.; Sowers, L. C., Characterization of DNA glycosylase activity by matrix-assisted laser desorption/ionization time-of-flight mass spectrometry. *Anal. Biochem.* **2009,** *394*, 13-23.
73. Sarhan, S.; Seiler, N., On the subcellular localization of the polyamines. *Biol. Chem. Hoppe Seyler* **1989,** *370* (12), 1279-1284.
74. Iacomino, G.; Picariello, G.; Sbrana, F.; Di Luccia, A.; Raiteri, R.; D'Agostino, L., DNA is wrapped by the nuclear aggregates of polyamines: the imaging evidence. *Biomacromolecules* **2011,** *12* (4), 1178-1186.
75. Raspaud, E.; Chaperon, I.; Leforestier, A.; Livolant, F., Spermine-induced aggregation of DNA, nucleosome, and chromatin. *Biophys. J.* **1999,** *77* (3), 1547-1555.
76. Pegg, A. E., Functions of Polyamines in Mammals. *J. Biol. Chem.* **2016,** *291* (29), 14904-12.
77. Johnston, R. F.; Pickett, S. C.; Barker, D. L., Autoradiography using storage phosphor technology. *Electrophoresis* **1990,** *11* (5), 355-360.
78. Hartley, J. A.; Souhami, R. L.; Berardini, M. D., Electrophoretic and chromatographic separation methods used to reveal interstrand crosslinking of nucleic acids. *J. Chromatog.* **1993,** *618*, 277-288.
79. Guan, L.; Greenberg, M. M., DNA interstand cross-link formation by the 1,4-dioxobutane abasic site. *J. Am. Chem. Soc.* **2009,** *131*, 15225-15231.
80. Sczepanski, J. T.; Jacobs, A. C.; Majumdar, A.; Greenberg, M. M., Scope and mechanism of interstrand crosslink formation by the C4'-oxidized abasic site. *J. Am. Chem. Soc.* **2009,** *131*, 11132-11139.
81. Fromme, J. C.; Verdine, G. L., Structure of a trapped endonuclease III-DNA covalent intermediate. *EMBO J.* **2003,** *22* (13), 3461-3471.
82. Gallopo, A. R.; Cleland, W. W., Properties of 3-hydroxypropionaldehyde 3-phosphate. *Arch. Biochem. Biophys.* **1979,** *195* (1), 152-154.
83. Bender, M. L.; Williams, A., Ketimine intermediates in amine-catalyzed enolization of acetone. *J. Am. Chem. Soc.* **1966,** *88* (11), 2502-2508.
84. Langenbeck, W.; Sauerbier, R., Organic catalysts. XVII. The hydration of crotonaldehyde to aldol. *Chem. Ber.* **1937,** *70, 1540*, 1540-1.
85. Paras, N. A.; MacMillan, D. W., The enantioselective organocatalytic 1,4-addition of electron-rich benzenes to alpha,beta-unsaturated aldehydes. *J Am Chem Soc* **2002,** *124* (27), 7894-5.
86. Enders, D.; Wang, C.; Liebich, J. X., Organocatalytic Asymmetric Aza-Michael Additions. *Chem. Eur. J.* **2009,** *15* (42), 11058-11076.
87. Luce, R. A.; Hopkins, P. B., Chemical cross-linking of drugs to DNA. *Methods Enzymol.* **2001,** *340*, 396-412.

88. Huang, H.; Hopkins, P. B., DNA interstrand cross-linking by formaldehyde: nucleotide sequence preference and covalent structure of the predominant cross-link formed in synthetic oligonucleotides. *J. Am. Chem. Soc.* **1993,** *115*, 9402-9408.
89. Stone, M. P.; Cho, Y. J.; Huang, H.; Kim, H. Y.; Kozekov, I. D.; Kozekova, A.; Wang, H.; Minko, I. G.; Lloyd, R. S.; Harris, T. M.; Rizzo, C. J., Interstrand cross-links induced by alpha, beta-unsaturated aldehydes derived from lipid peroxidation and environmental sources. *Acc. Chem. Res.* **2008,** *41*, 793-804.
90. Calow, A. D. J.; Carbó, J. J.; Cid, J.; Fernández, E.; Whiting, A., Understanding α,β-Unsaturated Imine Formation from Amine Additions to α,β-Unsaturated Aldehydes and Ketones: An Analytical and Theoretical Investigation. *J. Org. Chem.* **2014,** *79*, 5163−5172.
91. Sayre, L. M.; Arora, P. K.; Iyer, R. S.; Salomon, R. G., Pyrrole formation from 4-hydroxynonenal and primary amines. *Chem Res Toxicol* **1993,** *6* (1), 19-22.
92. Sako, M.; Yaekura, I., A convenient preparative method fo rthe 1,N2-cyclic adducts of guanine nucleosides and nucleotides with crontonaldehyde. *Tetrahedron* **2002,** *58*, 8413-8416.
93. Ollivier, N.; Agouridas, V.; Snella, B.; Desmet, R.; Drobecq, H.; Vicogne, J.; Melnyk, O., Catalysis of Hydrazone and Oxime Peptide Ligation by Arginine. *Org. Lett.* **2020,** *22* (21), 8608–8612.
94. Chung, F.-L.; Young, R.; Hecht, S. M., Formation of Cyclic 1,N2-Propanodeoxyguanosine Adducts in DNA upon Reaction with Acrolein or Crotonaldehyde. *Cancer Res.* **1984,** *44*, 990-995.
95. Winter, C. K.; Segall, H. J.; Haddon, W. F., Formation of cyclic adducts of deoxyguanosine with the aldehydes trans-4-hydroxy-2-hexenal and trans-4-hydroxy-2-nonenal in vitro. *Cancer Res.* **1986,** *46*, 56825686.
96. Lai, C.; Cao, H.; Hearst, J. E.; Corash, L.; Luo, H.; Wang, Y., Quantitative Analysis of DNA Interstrand Cross-Links and Monoadducts Formed in Human Cells Induced by Psoralens and UVA Irradiation. *Anal. Chem.* **2008,** *80* (22), 8790-8798.
97. Cao, H.; Hearst, J. E.; Corash, L.; Wang, Y., LC-MS/MS for the Detection of DNA Interstrand Cross-Links Formed by 8-Methoxypsoralen and UVA Irradiation in Human Cells. *Anal. Chem.* **2008,** *80* (8), 2932-2938.
98. Wang, Y.; Wang, Y., Structure elucidation of DNA interstrand crosslink lesions by a combination of nuclease P1 digestion with mass spectrometry. *Anal. Chem.* **2003,** *75*, 6306-6313.
99. Takenaka, K.; Kaneko, K.; Takahashi, N.; Nishimura, S.; Kakeya, H., Retro-aza-Michael reaction of an o-aminophenol adduct in protic solvents inspired by natural products. *Bioorg. Med. Chem.* **2021,** *35* 116059.
100. Yuan, Z.; Georgescu, R.; Bai, L.; Zhang, D.; Li, D.; O'Donnell, M. E., DNA unwinding mechanism of a eukaryotic replicative CMG helicase. *Nat. Commun.* **2020,** *11*, 688.
101. Morin, J. A.; Cao, F. J.; Lázaro, J. M.; Arias-Gonzalaz, R.; Valpuesta, J. M.; Carrascosa, J. L.; Salas, M.; Ibarra, B., Active DNA unwinding dynamics during processive DNA replication. *Proc. Nat. Acad. Sci. USA* **2012,** *109* (21), 8115-8120.
102. Yang, Z.; Johnson, K. M.; Price, N. E.; Gates, K. S., Characterization of interstrand DNA-DNA cross-links derived from abasic sites using bacteriophage φ29 DNA polymerase. *Biochemistry* **2015,** *54*, 4259-4266.

103. Semlow, D. R.; Zhang, J.; Budzowska, M.; Drohat, A. C.; Walter, J. C., Replication-dependent unhooking of DNA interstrand cross-links by the NEIL3 glycosylase. *Cell* **2016,** *167*, 498-511.
104. Whitaker, A. M.; Freudenthal, B. D., APE1: A skilled nucleic acid surgeon. *DNA Repair* **2018,** *71*, 93-100.
105. Beard, W. A.; Horton, J. K.; Prasad, R.; Wilson, S. H., Eukaryotic base excision repair: New approaches shine light on mechanism. *Annu. Rev. Biochem.* **2019,** *88*, 137-162.
106. Whitaker, A. M.; Flynn, T. S.; Freudenthal, B. D., Molecular snapshots of APE1 proofreading mismatches and removing DNA damage. *Nat. Commun.* **2018,** *9*, 399.
107. Chou, K.-M.; Cheng, Y.-C., An exonucleolytic activity of human apurinic/apyrimidinic endonuclease on 3' mispaired DNA. *Nature* **2002,** *415*, 655-659.
108. Liu, T.-C.; Lin, C.-T.; Chang, K.-C.; Guo, K.-W.; Wang, S.; Chu, J.-W.; Hsiao, Y.-Y., APE1 distinguishes DNA substrates in exonucleolytic cleavage by space-filling. *Nat. Commun.* **2021,** *12*, 601.
109. Wilson, D. M. I., Properties of and Substrate Determinants for the Exonuclease Activity of Human Apurinic Endonuclease Ape1. *J. Mol. Biol.* **2003,** *330*, 1027-1037.
110. Chou, K.-m.; Cheng, Y.-c., The exonuclease activity of human apurinic/apyrimidinic endonuclease (APE1). *J. Biol. Chem.* **2003,** *278* (20), 18289-18296.
111. Bhagwat, M.; Gerlt, J. A., 3'- and 5'-Strand Cleavage Reactions Catalyzed by the Fpg Protein from Escherichia coli Occur via Successive β- and δ-Elimination Mechanisms, Respectively. *Biochemistry* **1996,** *35* (2), 659–665.
112. Behmoaras, T.; Toulmé, J.-J.; Hélène, C., A tryptophan-containing peptide recognizes and cleaves DNA at abasic sites. *Nature* **1981,** *292*, 858-859.
113. Chaudhuri, A. R.; Nussenzweig, A., The multifaceted roles of PARP1 in DNA repair and chromatin remodeling. *Nat. Rev. Mol. Cell Biol.* **2017,** *18*, 610-621.
114. Robu, M.; Shah, R. G.; Purohit, N. K.; Zhou, P.; Naegeli, H.; Shah, G. M., Poly(ADP-ribose) polymerase 1 escorts XPC to UV-induced DNA lesions during nucleotide excision repair. *Proc. Nat. Acad. Sci. USA* **2017,** *114* (33), E6847-E6856.
115. Ghosh, S.; Greenberg, M. M., Nucleotide excision repair of chemically stabilized analogues of DNA interstrand cross-links produced from oxidized abasic sites. *Biochemistry* **2014,** *53*, 5958-5965.
116. Sczepanski, J. T.; Jacobs, A. C.; Van Houten, B.; Greenberg, M. M., Double strand break formation during nucleotide excision repair of a DNA interstrand cross-link. *Biochemistry* **2009,** *48*, 7565-7567.
117. Caldecott, K. W., Single-strand break repair and genetic disease. *Nat. Rev. Genetics* **2008,** *9*, 619-631.
118. Nilsen, L.; Forstrom, R. J.; Bjoras, M.; Alseth, I., AP endonuclease independent repair of abasic sites in Schizosaccharomyces pombe. *Nucleic Acids Res* **2012,** *40* (5), 2000-9.
119. Burkovics, P.; Hajdu, I.; Szukacsov, V.; Unk, I.; Haracska, L., Role of PCNA-dependent stimulation of 3'-phosphodiesterase and 3'-5' exonuclease activities of human Ape2 in repair of oxidative DNA damage. *Nucleic Acids Res* **2009,** *37* (13), 4247-55.
120. Alvarez-Quilon, A.; Wojtaszek, J. L.; Mathieu, M. C.; Patel, T.; Appel, C. D.; Hustedt, N.; Rossi, S. E.; Wallace, B. D.; Setiaputra, D.; Adam, S.; Ohashi, Y.; Melo, H.;

Cho, T.; Gervais, C.; Munoz, I. M.; Grazzini, E.; Young, J. T. F.; Rouse, J.; Zinda, M.; Williams, R. S.; Durocher, D., Endogenous DNA 3' Blocks Are Vulnerabilities for BRCA1 and BRCA2 Deficiency and Are Reversed by the APE2 Nuclease. *Mol Cell* **2020,** *78* (6), 1152-1165 e8.
121. Caldecott, K. W., XRCC1 protein; Form and function. *DNA Repair* **2019,** *81*, 102664.
122. Price, N. E.; Li, L.; Gates, K. S.; Wang, Y., Replication and repair of a reduced 2'-deoxyguanosine-abasic site cross-link in human cells. *Nucleic Acids Res.* **2017,** *45*, 6486-6493.
123. Matsumoto, Y.; kim, K., Excision of Deoxyribose Phosphate Residues by DNA Polymerase beta During DNA Repair. *Science* **2005,** *269*, 699-702.
124. Schärer, O. D., Nucleotide excision repair in eucaryotes. *Cold Spring Harb. Perspect. Biol.* **2013,** *5*, a012609.

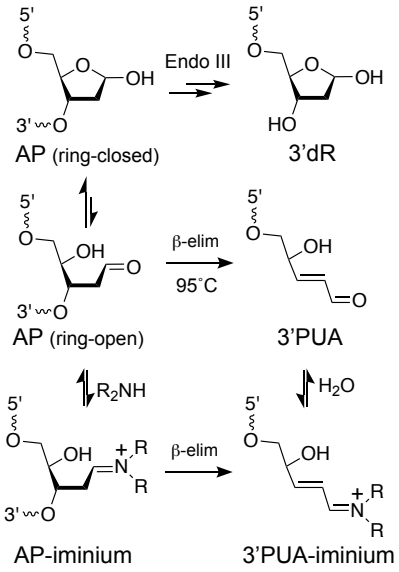

Scheme 1. β-Elimination at an AP site in DNA generates a strand break with an electrophilic α,β-unsaturated aldehyde or iminium ion sugar remnant on the 3'-terminus. The R groups on the amine catalyst represent either hydrogens or alkyl groups, depending on the identity of the amine.

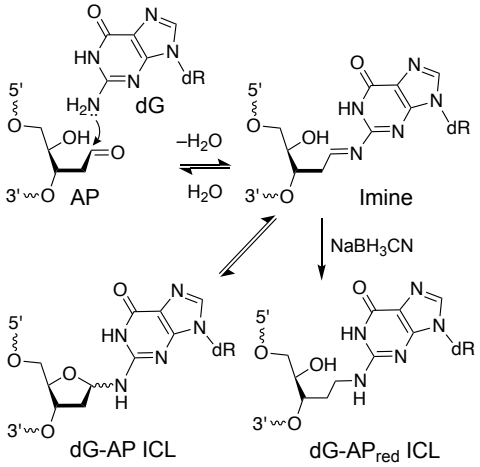

Scheme 2. The reaction of an intact AP site with a guanine residue on the opposing strand of duplex DNA generates a "full-size" ICL with two unbroken strands (duplex **B** in Figure 1 and Scheme 3 illustrates the architecture of this ICL). dR corresponds to the 2'-deoxyribose backbone of DNA attached to the guanine residue.

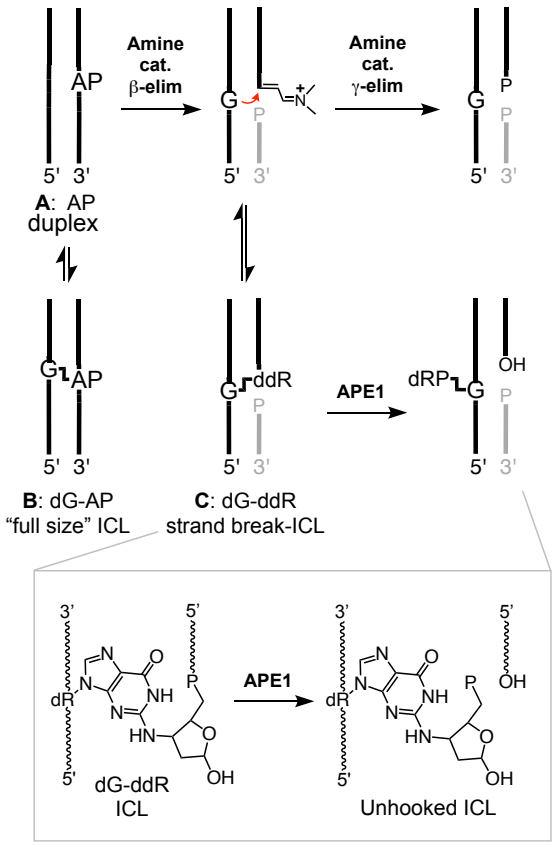

Scheme 3. Architectures of the full-size dG-AP ICL and the dG-ddR strand break/ICL generated from an AP-containing DNA duplex. The presence of a gray fragment indicates duplexes containing a strand break. The lower inset provides a molecular view of cross-link unhooking catalyzed by APE1. AP represents an abasic site, P represents a phosphoryl group, and dRP is a 2-deoxyribose-5-phosphate group.

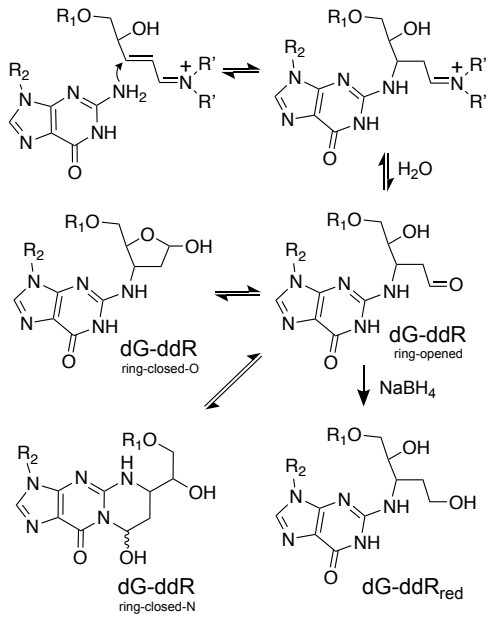

Scheme 4. Amine-catalyzed strand cleavage at an AP site in duplex DNA gives rise to a complex strand break/ICL via reaction of the α,β-unsaturated iminium ion intermediate with the N^2-amino group of a guanine residue on the opposing strand. R' represents H or alkyl groups associated with spermine and R_1 and R_2 = DNA.

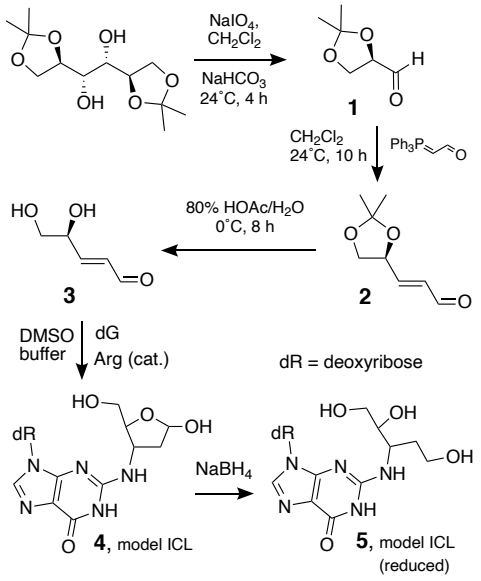

Scheme 5. A reaction modeling formation of the dG-ddR ICL identifies a fundamental chemical preference for conjugate addition of the exocyclic N^2-amino group of 2'-deoxyguanine to the electrophilic sugar remnant generated by strand cleavage at an AP site in DNA (dR represents the 2'-deoxyribose residue of 2'-deoxyguanosine, dG).

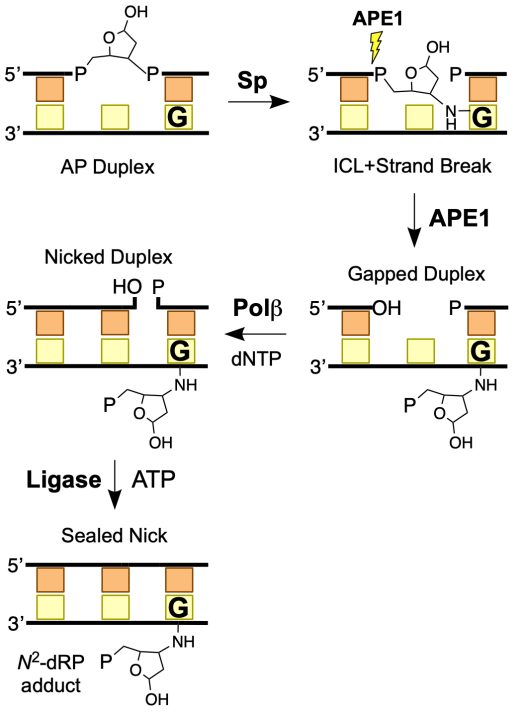

Scheme 6. Formation and unhooking of the dG-ddR ICL. Unhooking of the ICL by APE1 exposes a 3'OH group that enables repair of the lesion through a variant of the single-strand break repair pathway, involving gap-filling by polymerase β and sealing of the nick by DNA ligase. In this illustration, P represents a 5'-phosphoryl group or a phosphodiester linkage.

Figure 1

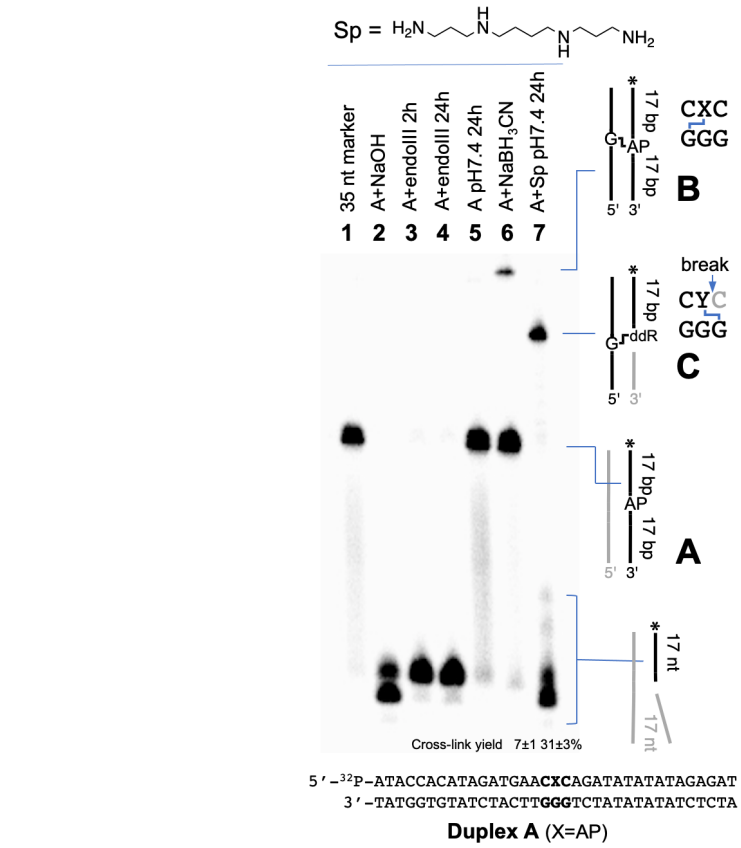

Figure 1. Gel electrophoretic evidence for an interstrand cross-link generated by spermine-catalyzed strand cleavage at the AP site in duplex A. Lane 1: 5'-^{32}P-labeled-AP-containing duplex **A**. Lane 2: The AP-containing duplex **A** treated with NaOH (165 mM, 37 °C, 30 min) to induce strand cleavage at the AP site, generating 3'P and 3'PUA cleavage products. Lane 3: AP-containing duplex **A** treated with Endo III (1 unit/μL) in a buffer composed of Tris-HCl (20 mM, pH 8), EDTA (1 mM), and DTT (1 mM) for 2 h at 37 °C to induce strand cleavage at the AP site, with corresponding generation of the 3'dR product. Lane 4: Duplex **A** treated with Endo III (1 unit/μL) in a buffer composed of Tris-HCl (20 mM, pH 8), EDTA (1 mM), and DTT (1 mM) for 2 h at 37 ℃ followed by ethanol precipitation of the DNA and incubation in HEPES (50 mM, pH 7.4) and NaCl (100 mM) at 37 ˚C for 24 h. Lane 5: The AP-containing duplex **A** incubated in HEPES (50 mM, pH 7.4) and NaCl (100 mM) at 37 ˚C. Lane 6: Duplex **A** incubated in sodium acetate buffer (pH 5.2, 750 mM) containing $NaBH_3CN$ (250 mM) at 37 ˚C for 24 h. Lane 7: Duplex **A** + spermine (Sp, 1 mM) in HEPES buffer (50 mM, pH 7, containing 100 mM NaCl) at 37 ˚C for 24 h. The ^{32}P-labeled oligodeoxynucleotides in the reactions were resolved by electrophoresis on a 0.4 mm thick 20% denaturing polyacrylamide gel and the radioactivity in each band quantitatively measured by storage-phosphor autoradiography. X = AP site, G-X = the dG-AP ICL, and G-Y = the G-ddR ICL (see Schemes 3 and 4 for chemical structures).

Figure 2

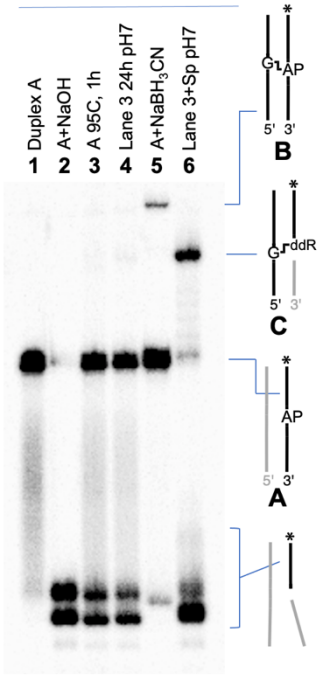

Figure 2. Evidence that the 3'PUA-iminium ion is the key intermediate involved in the spermine-catalyzed cross-link formation in duplex A. For structures of the 3'PUA iminium ion and 3'PUA cleavage products, see Scheme 1. Lane 1: 5'-^{32}P-labeled-AP-containing duplex **A**. Lane 2: The AP-containing duplex **A** treated with NaOH (165 mM, 37 ˚C, 30 min) to generate the 3'P and 3'PUA cleavage products. Lane 3: AP-containing duplex **A** heated at 95 ˚C for 30 min in HEPES buffer (50 mM, pH 7.4, containing 100 mM NaCl) to generate a mixture of intact AP site (45 %) alongside the 3'PUA (21 %) and 3'phosphate (24 %) cleavage products and then incubated for 1 h at 37 ˚C. Lane 4: Duplex **A** heated at 95 ˚C and then incubated at 37 ˚C for 24 h. Lane 5: size marker showing the "full-size" dG-AP$_{red}$ ICL generated by incubation of duplex **A** in pH 5.2 sodium acetate buffer (750 mM) containing $NaBH_3CN$ (250 mM) for 24 h at 37 ˚C. Lane 6: Duplex **A** heated at 95 ˚C for 30 min, followed by addition of spermine (Sp, 1 mM) and incubation in HEPES buffer (50 mM, pH 7.4, containing 100 mM NaCl) at 37 ˚C for 24 h. The ^{32}P-labeled oligodeoxynucleotides in the reactions were resolved by electrophoresis on a 0.4 mm thick 20% denaturing polyacrylamide gel and the radioactivity in each band quantitatively measured by storage-phosphor autoradiography.

Figure 3

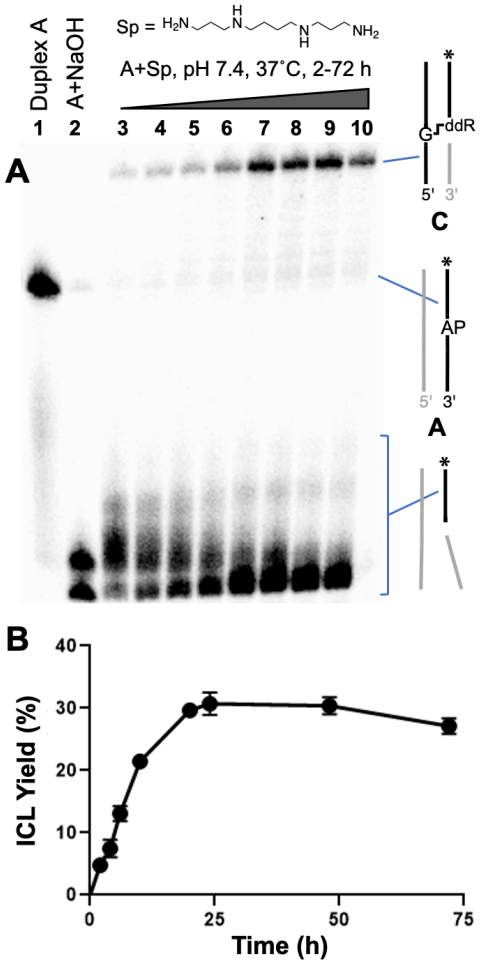

Figure 3. Time course for the formation of cross-linked DNA generated by amine-catalyzed cleavage of the AP site in duplex A. Panel A: Gel electrophoretic analysis of amine-catalyzed cross-link formation in duplex **A**. Lane 1: AP-containing duplex **A**. Lane 2: The AP-containing duplex **A** treated with NaOH (165 mM, 37°C, 30 min) to induce strand cleavage at the AP site, with generation of 3'P and 3'PUA cleavage products. Lanes 3-10: AP-containing duplex **A** was incubated with spermine (Sp, 1 mM) in HEPES buffer (50 mM, pH 7.4, containing 100 mM NaCl) at 37 ˚C. At prescribed time points aliquots were removed and frozen for subsequent gel electrophoretic analysis. The ^{32}P-labeled oligodeoxynucleotides in the reactions were resolved by electrophoresis on a 0.4 mm thick 20% denaturing polyacrylamide gel and the radioactivity in each band quantitatively measured by storage-phosphor autoradiography. Panel B: A plot of ICL yield versus time. The error bars reflect the standard deviation from three separate measurements.

Figure 4

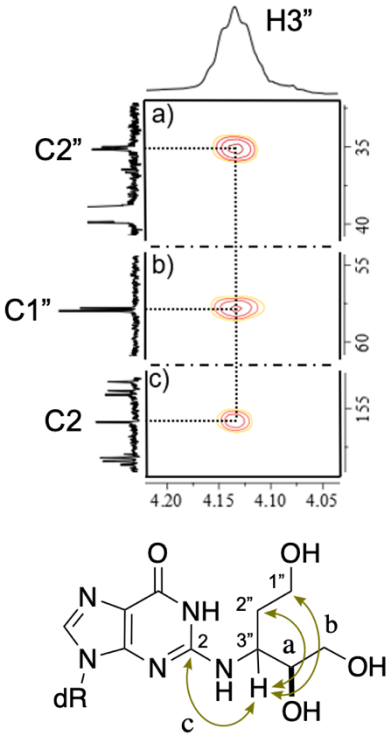

Figure 4. The structure of the model dG-ddR cross-link 5 was elucidated by 2D-NMR. Correlations between: (a) H3” and C2”, (b) H3” and C1” and (c) H3” and C2 in the ^{1}H-^{13}C HMBC spectra of the reduced model ICL **5** in DMSO-d_6 acquired at 600 MHz (^{1}H) and 151 MHz (^{13}C) were consistent with the model cross-link structure shown, arising from conjugate addition of the exocyclic N^2-amino group of dG with the α,β-unsaturated sugar remnant. Additional NMR spectral data are provided in Figures S9-S11.

Figure 5

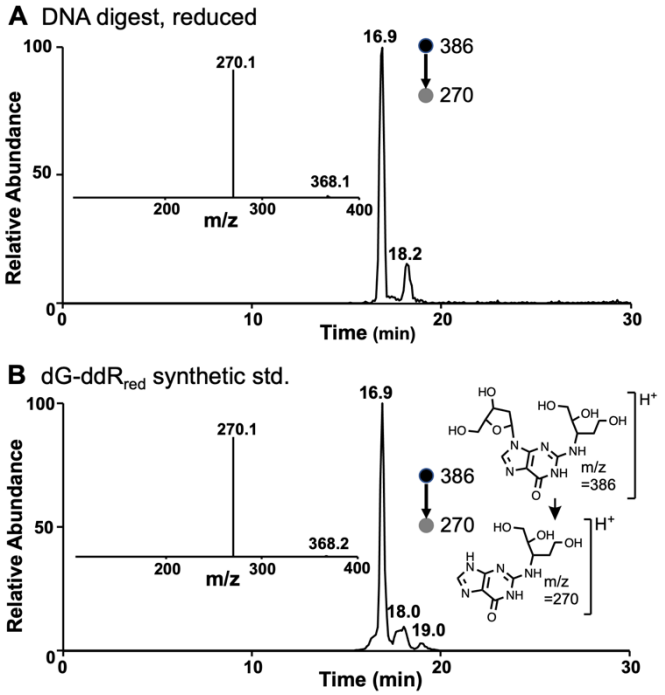

Figure 5. LC-MS/MS analyses establish the structure of the cross-link generated by amine-catalyzed strand cleavage in DNA duplex A. Panel A: Selected-ion chromatogram for monitoring the *m*/*z* 386→270 transition of the digest of cross-linked DNA generated by spermine-mediated strand cleavage of duplex **A**. Panel B: Selected-ion chromatogram for monitoring the *m*/*z* 386→270 transition which corresponds to the neutral loss of 2-deoxyribose of the synthetic standard of the reduced dG-ddR cross-link. The retention times and fragmentation patterns of the synthetic standard mirror that of the actual cross-link remnant obtained from digestion of $NaBH_4$-treated, cross-linked DNA. This provided evidence that the ICL in $NaBH_4$-treated DNA corresponds to the structure dG-ddR_{red} shown in Schemes 3 and 4. Additional results of LC-MS/MS/MS analyses for the reduced and unreduced cross-link are presented in Figure S13.

Figure 6

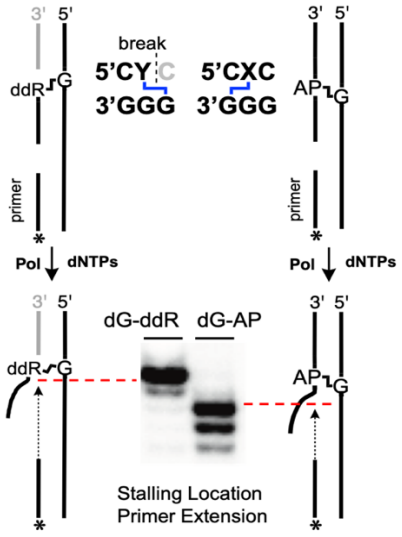

Figure 6. The dG-ddR ICL blocks DNA replication by the ϕ29 DNA polymerase. A 15 nt 5'-^{32}P-labeled primer was incubated with templates containing an ICL along with the polymerase enzyme (1 unit/μL), and the four dNTPs (1 mM in each) in Tris-HCl (50 mM, pH 7.5), $MgCl_2$ (10 mM), $(NH_4)_2SO_4$ (10 mM), DTT (4 mM), and bovine serum albumin (0.1 mg/mL) for 30 min at 24 °C. After reaction work-up, the primer extension products were analyzed on a 20% denaturing polyacrylamide gel. The gel image shows the locations where primer extension by the polymerase stalled on templates containing the dG-ddR and dG-AP_{red} ICLs. Complete sequences of the primer and templates are shown in Figure S1 and the complete gel electrophoretic analysis of primer extension reactions are shown in Figure S14. G-X is the dG-AP ICL and G-Y is the dG-ddR ICL (chemical structures are shown in Schemes 2-4).

Figure 7

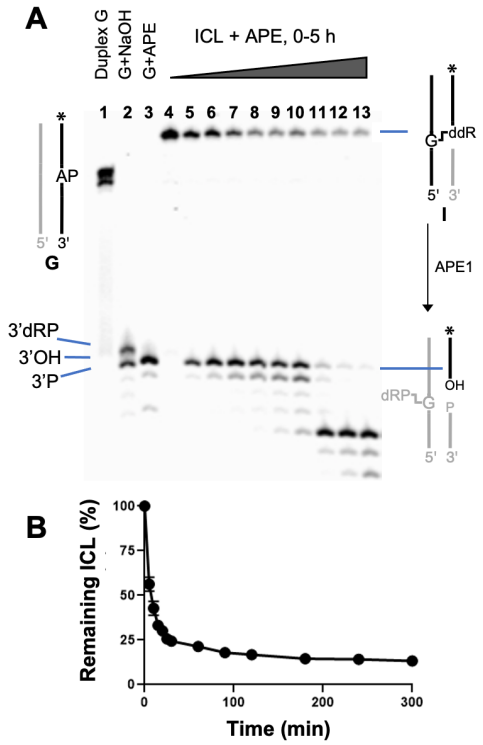

Figure 7. Unhooking of the dG-ddR ICL by the DNA repair enzyme apurinic endonuclease (APE1). The cross-linked DNA generated by amine-catalyzed cleavage of the AP site in duplex **G** was isolated by gel electrophoresis and annealed with a complementary 5'-phosphorylated oligonucleotide to generate the gapped substrate **I** (the complete sequences for these duplexes are shown in Figure S1). The gapped ICL was incubated with APE1 (2 units/μL) in Tris buffer (20 mM, pH 7.4) containing $MgCl_2$ (0.1 mM) and NaCl (20 mM) at 37 ˚C. At prescribed times aliquots were removed and frozen for subsequent gel electrophoretic analysis. The 5'-^{32}P-labeled oligodeoxynucleotides in the reactions were resolved by electrophoresis on a 0.4 mm thick 20% denaturing polyacrylamide gel and the radioactivity in each band quantitatively measured by storage-phosphor autoradiography. The initial unhooking product has gel mobility consistent with the 3'OH product. The smaller, faster-migrating products that become more prominent over time arise from further 3'-exonuclease activity of APE1 on the initial 3'OH product. Panel A shows the gel electrophoretic analysis of the enzymatic unhooking reaction and Panel B shows a plot of the unhooking of cross-linked DNA as a function of time. The error bars reflect the standard deviation from three separate experiments.

Figure 8

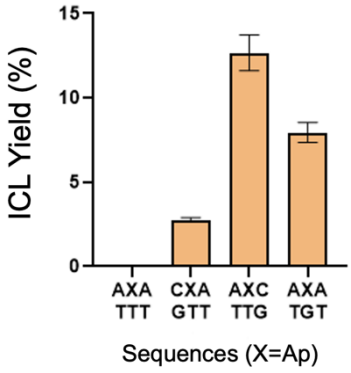

Figure 8. Yield of ICL resulting from amine-catalyzed strand cleavage of an AP site in various sequence contexts. The trinucleotide sequences shown were located in a sequence analogous to duplex **A**.

TOC Graphic

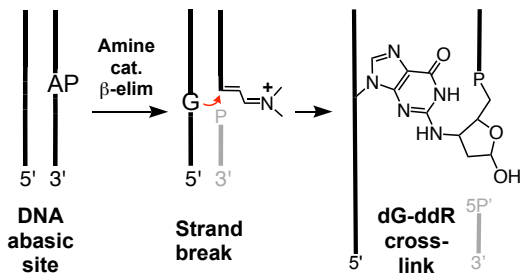
AP
Amine
cat.
β-elim
G
P
5'
3'
5'
3'
DNA
abasic
site
Strand
break
N
O
N
NH
N
HN
P
O
OH
5'
dG-ddR
cross-
link
5P'
3'